Mechanical and leakage behaviour of the dentin – adhesive interface

FRANCESCO MOLLICA
Department of Materials Engineering, University of Ferrara, Via Saragat 1, 44100 Ferrara, Italy
ROBERTO DE SANTIS*, LUIGI AMBROSIO, LUIGI NICOLAIS
Institute of Composite and Biomedical Materials, National Research Council, Piazzale Tecchio 80, 80125 Napoli, Italy
E-mail: rosantis@unina.it
DAVIDE PRISCO, SANDRO RENGO
University of Naples ''Federico II'', School of Dentistry, Via Pansini 5, 80100 Naples, Italy

Dentine bonding systems (DBS) have been developed in order to bond restorative materials (i.e. composite) to the inner walls of the tissues when function and integrity as to be restored. Adhesion to dentine results from the penetration of DBS into the demineralised substrate constituted by a swollen collagen network. The short-term stability of a restored tooth is mainly affected by the presence of defects which act as stress raiser, while the long-term stability of a restored tooth is mainly affected by the seal of the restorative material on the dental structures.

In order to determine the properties of the material interface, bonding to dentine is analysed using micro-tensile static and dynamic tests, assisted by the finite element modelling (FEM) and by the X-ray computed microtomography (micro-CT). The effect of voids and porosity in the composite layer of the DBS on the stress distribution has been investigated. Tensile adhesive strength for a particular DBS was measured on cylindrical specimens. The dual energy absorption technique, with the synchrotron beam light, has been developed to investigate, in a non-destructive manner, the leakage at the dentine–DBS interface of a silver nitrate staining solution as a function of mechanical cycling. The results indicate that leakage occurs radially through the dentine–adhesive interface and is influenced by the porosity in the adhesive and composite layers.

Introduction

Filler reinforced polymers for tooth reconstruction is increasing because of the interesting coupling between aesthetic and mechanical properties of these composite materials [1, 2]. Dentine bonding systems (DBS) have been developed in order to bond restorative materials (i.e. composite) to the inner walls of the tissues when function and integrity as to be restored [3, 4]. Several removal and conditioning methods have been developed [5] in order to increase the retentive capacity of the substrate, in particular, the acid-etching technique is commonly used in order to remove the debris layer (smear layer), reopen the dentinal tubules and demineralise the upper layer of dentine [6–11]. Adhesion to dentine results from the penetration of DBS into the demineralised substrate constituted by a swollen collagen network [12–15]. The main mechanism of adhesion between dentine and DBS is micro-mechanical interlocking, while chemical bonding is the main adhesion mechanism between DBS and the composite restorative material [16–18].

The research on interfaces between biological and non-biological entities is of primary importance for the development of new techniques and new advanced materials in medical applications requiring the substitution of mineralised hard tissues such as dentine and bone. The short-term stability of a restored tooth is mainly affected by the presence of defects which act as stress raiser, while the long-term stability of a restored tooth is mainly affected by the seal of the restorative material on the dental structures. The passage of low-molecular-weight fluids through the interface between the restoration and the tooth structures leads to infiltration of bacteria from the oral environment into dentin, and this in turn is cause of secondary caries with subsequent pulp pathology and failure [11, 23] and can even lead to the degradation of the resin–dentine bonds [24]. This phenomenon is known as leakage and, according to the

*Author to whom all correspondence should be addressed.

0957–4530

size characterising the phenomenon, the terms ''micro-leakage'' and ''nano-leakage'' are also commonly used. Investigation on leakage at the interface between restoration and dental tissues is of great importance and concern in dentistry.

Although the acid-etching technique inhibits leakage at the enamel–restoration interface and improves dentine–restorative material bonding strength, it is not so satisfactory in terms of sealing the dentine–restorative material interface [11, 15–17, 25, 26], thus leakage at the dentine margins of the cavities yet remains an unsolved problem. In fact, DBS obtained with the ''total-etch'' technique are able to form apparent gap-free margins at the dentine–restoration interface, but it has been found [27] that leakage along the dentinal wall is still evident. This may be due to permeation through the hybrid layer as the result of an incomplete infiltration of the adhesive into the demineralised dentine. The quality of the dentine bond was reported to depend on the chemistry of the individual DBS in certain situations. The microstructure plays also an important role on the behaviour of the interface, thus detailed information is needed on the mechanisms guiding the development of the hybrid system.

Almost all the research on leakage patterns along gap-free margins is carried out for several bonding systems using *in vitro* measurement of marker fluids (i.e. methylene blue or silver nitrate solutions) leakage through the dentine–restorative materials interface followed by either visual imaging or imaging through scanning electron microscopy (SEM) or transmission electron microscopy (TEM) [27–32]. Silver nitrate solution staining is one of the most commonly used methods for microleakage evaluation. Compared with other staining techniques, silver staining provides a much sharper SEM picture of penetration at tooth–restoration margins [33].

The major disadvantage of traditional SEM investigations is that they are essentially surface measurements. Although 3-D data can be obtained through serial sectioning, this is a destructive testing technique, thus the analysis of the kinetics of the problem is extremely difficult, especially when correlation to thermal cycling and/or dynamic mechanical loading is sought. Moreover the sectioning of a residually stressed material system provides specimens which may undergo recovery due to the lack of stress transmitted at the boundary with the removed part, and this can lead to serious mistakes in the determination of geometric features of the specimen. What is needed, then, is a technique that is able to yield non-destructive 3-D information on the microstructure of materials.

X-ray micro CT is a possible answer to this need. A set of planar images of the object at several orientation with respect to the X-ray source is first collected then fed into a computer programme which produces a 3-D reconstruction of the sample. The unique feature of the X-ray micro-CT is that the 3-D reconstruction, which consists of multi-sliced tomographs taken in a fine pitch along a vertical rotational axis, can be sliced along any direction to gain an accurate information on the internal spatial properties of the object. Therefore, 3-D images of the tissue may be developed with a few micron resolution [34], from which structural quantities can be derived. Synchrotron radiation for 3-D imaging is now routinely used on several beamlines to perform investigations on a wide range of materials [35, 36]. Characteristics of the synchrotron beam light are coherence, high spatial resolution and the real time combination of techniques.

In classical mechanical tests, such as tension, compression, torsion, bending, etc., performed on connective mineralised hard tissues, a minimum cross-sectional area of 4 mm^2 is sufficient: in the case of bone, such specimens contain various haversian systems [37] and thus provide significant data. Unfortunately, this cross-section value is too small to be reached by an average dentine specimen, thus an adequate characterisation of dentin and DBS with classical tests is very difficult. Reduced minimum cross-sectional values can be achieved in micro-mechanical tests [38–42], which are commonly used for the characterisation of the mechanical anisotropy of living hard connective tissues, such as bones and dentine. It is advisable, though, to use the finite element modelling (FEM) as a powerful tool to support the experimental test, in order to carefully check the stress distribution in non-standardised specimens and in presence of complex geometries [43–49].

In this study micro-mechanical tests are performed on dentin specimens treated with an alcohol-based DBS. Micro-tensile static and dynamic tests, assisted by the finite element modelling (FEM) and by the X-ray micro-CT, are used to determine the relationship between material design, structure and properties. A non-destructive method (the dual energy absorption technique with the synchrotron beam light) has been used to investigate the leakage of silver nitrate staining at the dentine–DBS interface as a function of mechanical cycling. The proposed combined approach has a higher probability to give significant information because the experimental (static and fatigue tests), numerical (FEM) and imaging (X-ray micro-CT) methods, used together and in parallel, are of greater value than either technique used alone.

Materials and methods

Thirty selected sound third human molars have been used. Teeth specimens are embedded into hollow stainless steel cylinders ($\phi_e = 16.0$ mm; $\phi_i = 14.0$ mm; $h = 20.0$ mm) using PMMA-based cements [50, 51]. The position of the tooth in the stainless steel frame is driven by commercial planar X-ray radiography showing the gross image of the region of interest (Fig. 1(a)). The coronal tooth is cut with a water-cooled low-speed diamond saw (Isomet Buehler Low Speed Saw), leaving about 3.5 ($\pm$ 0.5) mm) between the free dentine surface and the pulpal roof. Each specimen is then gripped in the chuck of a water cooled lathe and a standardised cylinder of dentine ($\phi = 4.0$ mm) is obtained, whose axis is perfectly coincident with that of the external stainless frame [34, 51]. Waterproof abrasive paper in the range of grits from #600 to #1000 is used in order to simulate the smear layer on the free flat surface (a disc with a diameter less or equal to 4 mm, Fig. 1(b)) of the specimen. The

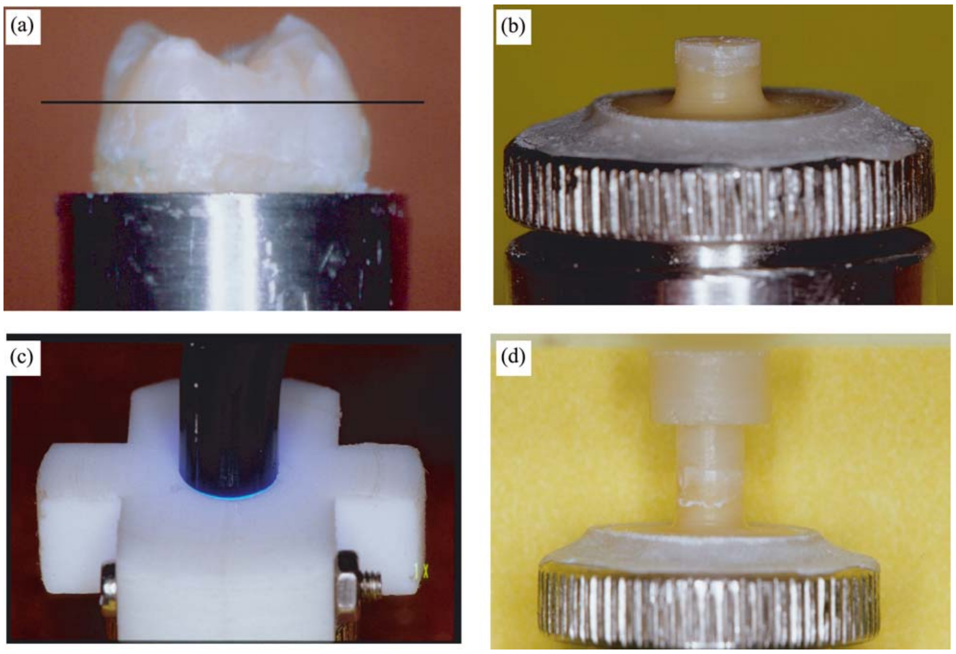

Figure 1 Specimen preparation.

acid-etching technique proposed by Buonocore [6] is used to remove the smear layer; dentine is etched for 30 s using 37.5% phosphoric acid gel (Kerr Gel Etchant).

The bonding system composed of Amelogen Universal® composite and PQ1 Permaquick® (Ultradent, South Jordan, USA) adhesive is applied on the etched surface according to the manufacturer's instructions, in the following way. Teflon moulds coupled to the lateral cylindrical dentine surface (Fig. 1(c)) are used to realise a cylindrical cavity, closed at one side by a free dentine surface. Here, the adhesive and the composite are sequentially applied and light polymerised through a layer by layer stratification (each layer is about 2 mm thick). The polymerisation of both the adhesive and the composite systems (Fig. 1(c)) is obtained by using an Optilux halogen lamp (400 mW/cm^2 for 60 s). The mould is then removed and the result is a cylindrical specimen, dumbell or dog-bone shaped, characterised by a dentine–adhesive–composite interface in its middle cross-section (Fig. 1(d)), the bottom and the upper part of this hybrid layer are dentine and composite, respectively. The unique feature of this specimen is its axial symmetry, which facilitates mechanical stress computations at the interface and X-ray tomography as well. The specimen is now ready to be mechanically tested with a dynamometer in tension or torsion, and the simple geometrical shape facilitates 3-D scan devices, an accurate measurement of the bonding strength, numerical analyses (FEM) and imaging.

Mechanical static tests in tension are performed using an Instron 4204 screw driven dynamometer at a cross-head speed of 0.5 mm/min and with a loading cell of 1 KN at room temperature. The strain is monitored with an MTS extensometer (MTS 632,32 F), load, displacement and strain measurements are acquired at a rate of 20 points/s. Twenty of the thirty specimens are used for the static characterisation. Fig. 2 shows the static mechanical set-up test, particularly the extensometer arm is designed in order to provide high resolution output with very low

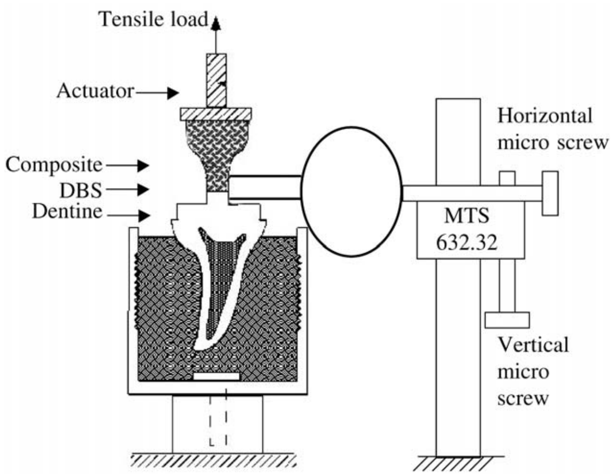

Figure 2 Mechanical static test set up.

contact forces. The static tensile tests yields results in the form of the stress–strain curve, in which the strain is directly provided by the extensometer and the stress is computed, as usual, by dividing the load measured by the loading cell by the initial cross-sectional area. The statistical significance of the results was assessed using the one-way ANOVA variance test [52]. However, since the mechanical behaviour is rather brittle, the Weibull distribution [53, 54] is used to compute the failure probability F as a function of the applied stress σ:

$$F(\sigma) = 1 - e^{-\left(\frac{\sigma}{\sigma_0}\right)^m}$$

where σ_0 and m are two material parameters that provide the spread of the failure data with respect to the stress axis and represent the characteristic strength and slope of the distribution function, respectively.

In order to obtain information on the dynamic properties of the interface, fatigue tests are carried out on the remaining 10 specimens at a frequency of 2 Hz, which is an average frequency of chewing. A suitable choice for the conditions of the dynamic testing (i.e. mean stress and amplitude) is suggested by the results of the static test. The fatigue tests are performed in an environmental chamber with the temperature controlled by a thermostatic heater (Techne TE10D, Cambridge, UK), and specimens have been kept in water at room temperature prior to testing to prevent dehydration. In order to investigate the mechanical effect on the sealing capability of the DBS, the selected dentin–composite specimens undergo fatigue cycling in a 50% $AgNO_3$ solution. The Ag^+ ions in the solution are able to penetrate the small gaps at the interface between dentin and DBS, where they precipitate forming small inclusions of metallic Ag, which can be easily visualised through X-ray irradiation. In order to visualise only the extent of penetration, the dual energy X-ray micro-CT investigation technique is used: two sets of imaging data are collected, one using X-rays, whose energy is slightly above the absorption edge of the element of interest (Ag) and the other one just below the same absorption edge. The contrast, which can be seen with the difference between the two sets of data is almost entirely due to the absorption of the element of interest, which is thus clearly visualised. The principal advantage of this technique is the non-destructive nature of the method, while the main limitation is the range of infiltrating elements which can be used, since their absorption edge must be within the energy range of the beamline. The lateral surface of the dentin cylinder is coated with acrylic resin (nail polish) in order to prevent leakage through this surface.

Concerning the sealing ability of the restorations and the quality of the hybrid layer, two specimens are loaded with fatigue cycles between 1 and 5 MPa in a 50% $AgNO_3$ solution up to 10 000 and 100 000 cycles respectively, while two more specimens, used as controls, were kept at rest in the same environment for 1, 5 and 15 h, respectively. The diffusion of Ag^+ ions through the interface is then analysed through time as a function of the material, its application technique, the number of cycles and the amplitude/mean stress. The X-ray imaging was performed at the SYRMEP beamline at ELETTRA, Trieste, Italy), where a different method of obtaining quantitative elemental information from X-ray microtomography, the dual energy microtomography, has been developed [55].

The finite element method (FEM) has been used to run simulations of the static mechanical tests. This is necessary in order to check that the state of stress at the two interfaces (dentine–adhesive and adhesive–composite) is indeed uniform, so that the stress on the interfaces can be calculated by dividing the applied force by the area of the cross-section correctly. For instance, the presence of the pulpal chamber is an element that can perturb the stress distribution, so that the state of stress can no longer be considered uniform. To this end, a model of a generic specimen, which includes a generic pulpal chamber, has been analysed and it is possible to conclude that the influence of the pulpal chamber is negligible. The results of such an analysis will be published elsewhere.

Results and discussion

Static stress–strain diagrams showed a linear behaviour up to rupture. The mean values and the standard deviations of the stress and strain at failure as well as the mean slope of the stress–strain curves are 16.06 MPa (5.72 MPa), 0.18% (0.06%) and 9.97 GPa (3.4 GPa) respectively. In the analyses we excluded the specimens which underwent a cohesive failure at the pulpal roof. The slope of the stress–strain diagram represents the stiffness of the specimen, hence it is an average elastic modulus of the series of materials between the arm of the extensometer, i.e. dentine, hybrid layer and composite. Since the hybrid layer thickness is negligible if compared to the gauged length of dentine and composite (about 2 mm), the contribution of the interface to the compliance of the system is negligible, thus the measured slope becomes an average Young's modulus between dentine and composite. It can be easily concluded that the spreading of the measured slope mainly depends on the Young's modulus of dentine, which varies between 10 and 20 GPa [8], and the position of the extensometer arms across the hybrid layer. This variability is reflected in the standard deviations of both the slope and the ultimate strain, while the stress measurements are independent of the specimen's gauge length.

The linear stress strain curves up to rupture and the consequent rapid failure of the interface suggest that the behaviour of the tested materials is brittle. Fig. 3 shows the mean stress–strain curve and the Weibull plot for the dentine–DBS–composite axial strength. The Weibull distribution parameters and their respective standard errors are $m = 3.53$ (0.28) and $\sigma_0 = 16.55$ MPa (0.27 Mpa). Moreover the sum of the squared errors between the original data and the calculated curve fit (i.e. χ^2) and the linear correlation coefficients (R) are 0.05 and 0.98, respectively. In general, the lower the χ^2 value, the better the fit, while the correlation coefficient indicates how well the calculated curve fits the original data, thus providing a measure of the ''alignment'' of the distribution. An R value above 0.9 is generally considered as acceptable.

The X-ray micro-CT images are also used to evaluate the quality of the specimen preparation and the interface between dentine and DBS-composite. Particularly Fig. 4 shows a planar X-ray longitudinal image before mechanical and leakage testing and the dentine, DBS and composite can be detected. The most important feature that can be seen in the reconstructed images is the presence of porosity (Fig. 5). In fact, pseudospherical

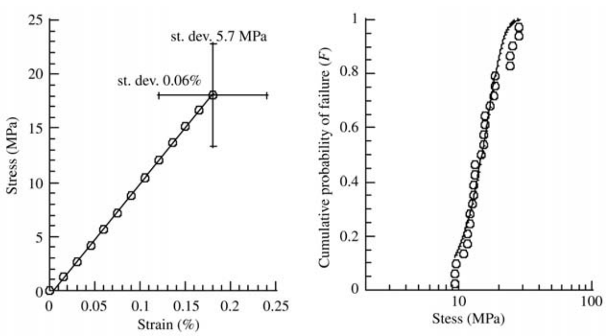

Figure 3 Stress–strain and Weibull plots for the investigated DBS system.

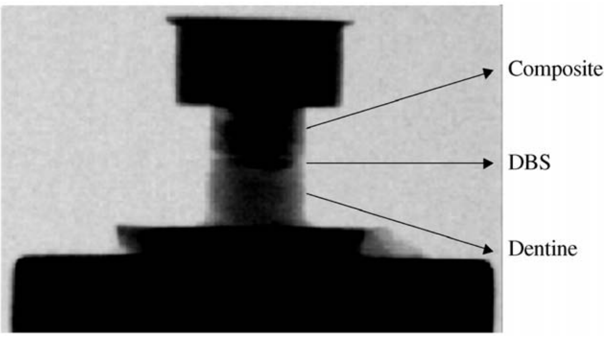

Figure 4 X-ray planar image of dentin–DBS–composite system.

voids are present in the adhesive layer and in the composite layer close to the interface with the adhesive, especially in the region close to the external lateral surface. On the other hand, dentin and the composite far from the interface are relatively void free. Clinically, adhesive systems should be in place for a significant time, and more importantly, completely seal the restoration margins [3]. Instead, increased porosity at the bonded interface over time in clinical trials of bonded restoration is largely documented. Silver ion accumulations in silver nitrate staining micro-leakage evaluation were often noted at the base of the hybrid layer for all materials [27, 56]. This leakage occurred within the demineralised dentine indicating that adhesive systems do not completely permeate the demineralised dentine, but leave a hybrid layer with large amounts of porosity which may subsequently allow dentinal or oral fluid to slowly diffuse through the interface and subsequently hydrolyse the adhesive resin and collagen [15, 27]. A gradual transition of resin concentration in the demineralised superficial dentine has been found; the concentration of resin was greatest at the top of the hybrid layer and lowest near the base [32], If resin does not penetrate to the full depth of the demineralised zone, the un-infiltrated weak collagen layer at the base of the zone may be susceptible to long-term hydrolytic degradation. The ideal penetration of resin into the hybrid layer may not always be achieved due to the residual water content of the collagen after etching, collapse of the collagen network, incomplete resin infiltration, and/or incomplete resin polymerisation [57].

The presence of porosity in the DBS, thus, may be unavoidable also in clinical practice, therefore it is important to evaluate its influence on the mechanical properties of the specimens. To this end, a specimen with one representative lenticular void, located in the peripheral region of the composite close to the composite–adhesive interface has been modelled with the commercial FEM software ANSYS Mechanical 5.7® (Ansys Inc., Canonsburg, PA, USA). Using the symmetry, only half of the geometry needed to be drawn. The model is then meshed using 10 node tetrahedral elements, which are convenient in this case, due to the complexity of the shape of the model (Fig. 6). The mesh was adequately refined at the locations of

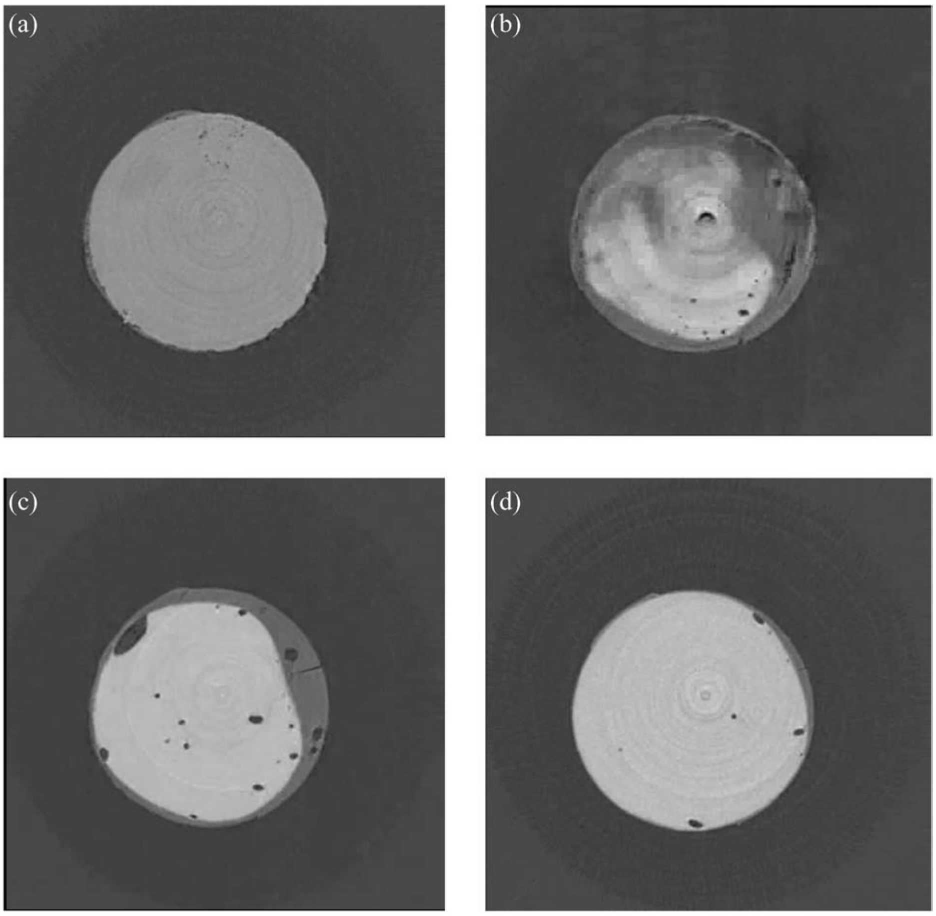

Figure 5 Details of the cross section: (a) dentin, (b) adhesive, (c) composite near the adhesive interface, (d) composite far from the interface. Porosity is particularly evident in (b) and (c).

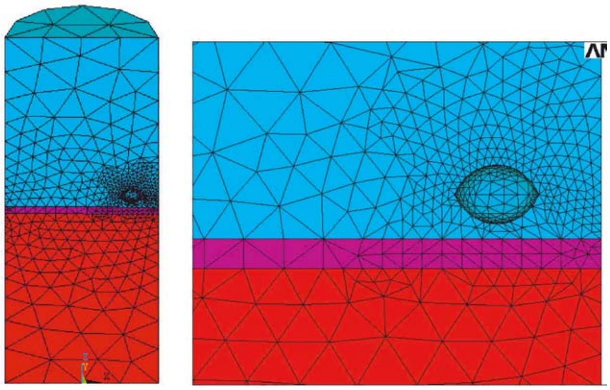

Figure 6 The FEM mesh of the whole specimen and the detail with the lenticular void.

TABLE I Number of cycles to failure as a function of the applied dynamic load. (*) indicates specimens which cycled in $AgNO_3$ solution without breaking

Load (N)	Number of cycles to failure
50	200 000
50	72 800
50	$10^5(*)$
50	$10^5(*)$
60	82 700
70	75 500
70	$10^4(*)$
70	$10^4(*)$
100	1080
120	120

expected maximum displacement gradients in order to improve accuracy. In particular, refinement was performed close to line fillets and to the void (geometrical discontinuities) and close to the two interfaces (material discontinuities), as can be seen from Fig. 6. The model produced about 5000 elements, which were loaded simulating the simple tension tests with a vertical load of 10 MPa. Dentine, adhesive and composite are assumed to have a modulus of 15, 1 and 9 GPa respectively, all the materials are modelled as isotropic, homogeneous and linearly elastic with a Poisson's ratio of 0.33. Such an assumption is correct for the adhesive layer and partly for the composite, the reinforcement being in the form of particles which are randomly dispersed in the bulk of the material. In the case of dentine, though, the anisotropy due to dentinal tubules can hardly be modelled as an isotropic material. On the other hand, for the sake of simplicity a linearly elastic isotropic material to model dentine is adopted, using an average Young's modulus. The results of the FEM analysis are depicted in Fig. 7, where the von Mises stress distribution is shown in the region close to the void. The void determines a stress intensity factor of about 3.7. On the other hand the adhesive layer directly under the void is considerably unloaded. The presence of voids necessarily influences the fatigue resistance of the specimens and the leakage properties as well.

Table I indicates the cycles to failure as a function of the applied dynamic loading. In the same table specimens which cycled in $AgNO_3$ and specimens which sustained up to 1 million cycles without failure are also reported. Leakage of Ag^+ ions through the interface occurs as a result of the mechanical cycling. By using the dual sorption technique different leakage patterns may be distinguished at the margin of the interface, and Fig. 8 shows a cross-section reconstruction of the interface of a specimen which underwent 10^5 cycles at 50 N. At this

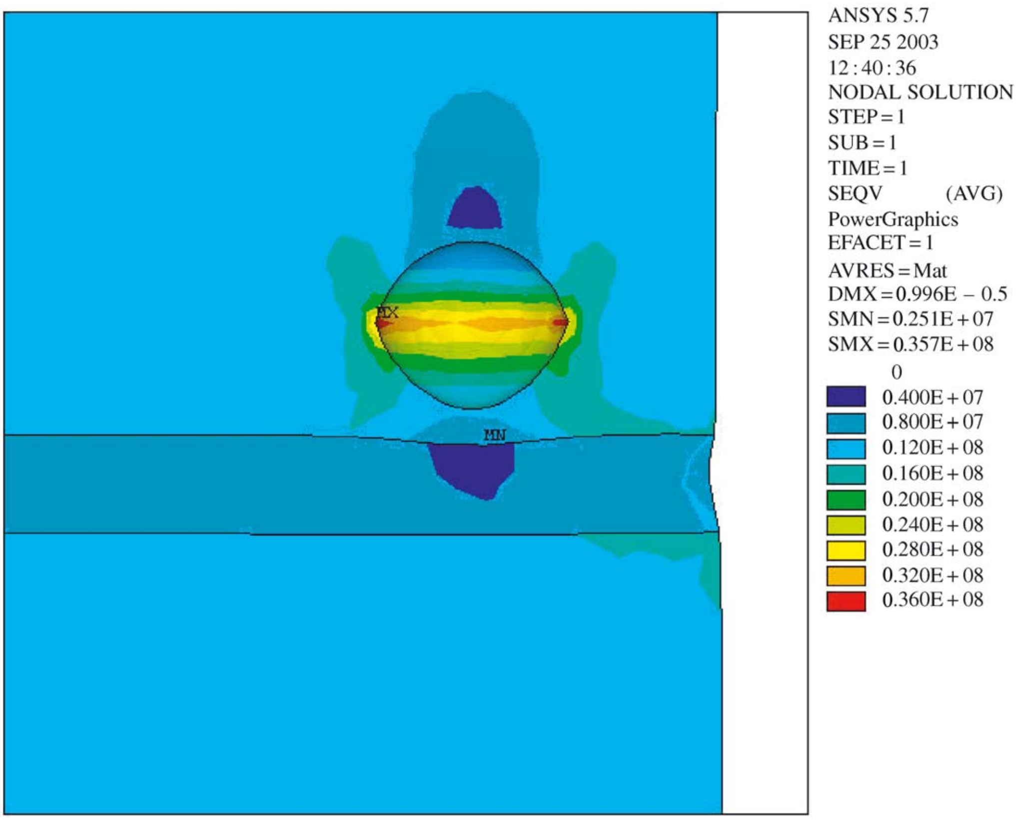

Figure 7 The von Mises stress distribution after an axial load of 10 MPa. The void acts as a stress raiser with stress intensity factor of about 3.7.

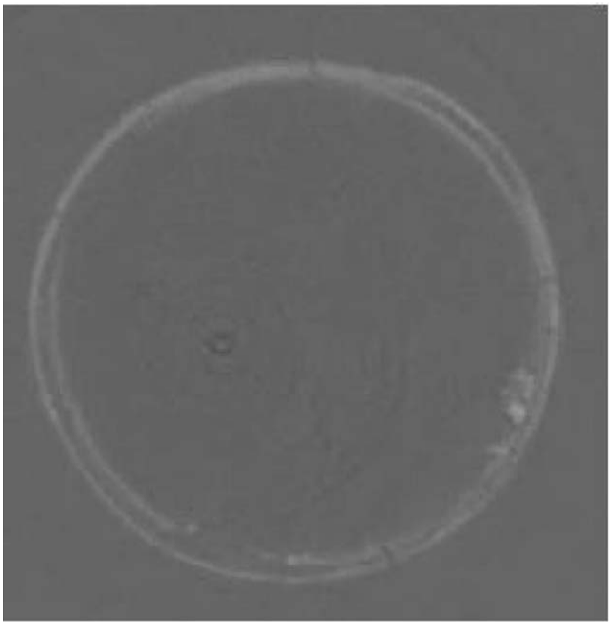

Figure 8 The difference between imaging data collected above and below the absorption edge of Ag for a specimen which underwent 10^5 cycles.

stress level and number of cycles this specimen shows a radial leakage which reaches depth up to 0.5 mm. Understandably, the presence of voids favours leakage, and this can be seen in the lower right comer of Fig. 8, where there is a slight departure from radial symmetry caused by one of such voids.

Conclusions

The simple geometrical shape of the specimens used in this investigation (Fig. 1) facilitates 3-D scan imaging (Fig. 8), numerical analyses (figure FEM), and an accurate measurement of the bonding strength (Fig. 3). Despite the limited number of specimens, we are confident with the results, since the statistical correlation coefficient showed values above 0.9, thus denoting a good correlation with the Weibull distribution.

The SEM investigations are bidimensional measurements, serial sectioning can provide 3-D data, but being a destructive technique, it does not allow direct studies on the diffusion dynamics. The X-ray dual sorption technique is a very powerful tool to investigate silver nitrate leakage at the dentine–DBS–composite interface, providing very sharp micro-CT images of the Ag^+ ions penetration at tooth–restoration margins. Moreover, the effect of cycling conditions on the staining depth penetration can be analysed in a non destructive manner. Although the acid-etching technique inhibits leakage at the enamel–restoration interface and improves dentine-restoration bonding strength, X-ray micro-CT investigation clearly shows that it is not so satisfactory in terms of sealing the dentine–restoration interface. Further investigations need to be carried out in order to assess the relationship between leakage and mechanical stress according to materials, substrate conditioning and techniques, moreover, other heavy staining elements, less invasive than silver nitrate [58], have to be considered.

Acknowledgments

This research was supported by the PRIN 2002 from MIUR prot. 2002-063819 and Centro di Competenze ''Nuove Tecnologie per attività di produzione'' Misura 316 POR 2000/2006. The authors are grateful to the Syrmep beamline of the synchrotron of ELETTRA (Basovizza, Trieste) for the micro-tomography imaging. The authors also wish to thank Dr Federica Di Stasio and Mr Rodolfo Morra for the mechanical testing.

References

1. S. RAMAKRISHNA, J. MAYER, E. WINTERMANTEL and K. W. LEONG, *Comp. Sci. Tech.* **61** (2001) 1189.
2. M. DONKERWOLCKE, F. BURNY and D. MUSTER, *Biomaterials* **19** (1998) 1461.
3. B. VAN MEERBEEK, J. PERDIGAO, P. LAMBRECHTS and G. VANHERLE, *J. Dent.* **26** (1998) 1.
4. A. TAKAHASHI, Y. SATO, S. UNO, P. N. R. PEREIRA and H. SANO, *Dent. Mater.* **18** (2002) 263.
5. A. R. YAZICI, G. OZGUNALTAY and B. DAYANGAC, *Oper. Dent.* **27** (2002) 360.
6. M. G. BUONOCORE, *J. Dent. Res.* **34** (1955) 846.
7. N. NAKABAYASHI, *Biomaterials* **24** (2003) 2437.
8. S. S. A. OLIVEIRA, S. J. MARSHALL, J. F. HILTON and G. W. MARSHALL, *ibid.* **23** (2002) 4105.
9. L. BRESCHI, P. GOBBI, G. MAZZOTTI, M. FALCONI, T. H. ELLIS and I. STANGEL, *Dent. Mater.* **18** (2002) 26.
10. R. S. HOBSON, A. J. RUGG-GUNN and T. A. BOOTH, *Arch. Oral. Biol.* **47** (2002) 407.
11. G. W. MARSHALL JR, S. J. MARSHALL, J. H. KINNEY and M. BALOOCH, *J. Dent.* **25** (1997) 441.
12. F. R. TAY, A. J. GWINNETT, K. M. PANG and S. H. Y. WEI, *J. Dent. Res.* **75** (1996) 1034.
13. F. R. TAY, A. J. GWINNETT and S. H. Y. WEI, *Am. J. Dent.* **9** (1996) 161.
14. F. R. TAY, A. J. GWINNETT and S. H. Y. WEI, *Dent. Mater.* **14** (1998) 329.
15. D. H. PASHLEY and R. M. CARVALHO, *J. Dent.* **25** (1997) 355.
16. N. NAKABAYASHI, K. KOJIMA and E. MASUHARA, *J. Biomed. Mater. Res.* **16** (1982) 265.
17. N. NAKABAYASHI and K. TAKARADA, *Dent. Mater.* **8** (1992) 125.
18. D. C. SMITH, in ''Biomaterials Science'' (Academic Press, San Diego, 1996) p. 319–325.
19. D. H. PASHLEY, *J. End.* **16** (1990) 70.
20. C. L. DAVIDSON and A. I. ABDALLA, *Am. J. Dent.* **7** (1994) 112.
21. B. CIUCCHI, S. BOUILLAGUET, M. DELALOYE and J. HOLZ, *J. Dent.* **25** (1997) 305.
22. C. BESNAULT and J. P. ATTAL, *J. Dent.* **30** (2002) 1.
23. J. CAMPS, J. DEJOU, M. REMUSAT and I. ABOUT, *Dent. Mat.* **1** (2000) 432.
24. M. HASHIMOTO, H. OHNO, H. SANO, M. KAGA and H. OGUCHI, *Biomaterials* **24** (2003) 3795.
25. N. KANEMURA, H. SANO and J. TAGAMI, *J. Dent.* **27** (1999) 523.
26. A. U. J. YAP, G. J. PEARSON, R. W. BILLINGTON and A. N. STOKES, *Biomaterials* **17** (1996) 2031.
27. H. SANO, T. TAKATSU, B. CIUCCHI, A. J. HERNER, W. G. MATTEWS and D. H. PASHLEY, *Oper. Dent.* **20** (1995) 18.
28. J. MANHART, H. Y. CHEN, A. MEHL, K. WEBER and R. HICKEL, *J. Dent.* **29** (2001) 123.
29. G. C. LOPES, M. FRANKE and H. P. MAIA, *J. Prost. Dent.* **88** (2002) 32.
30. H. SANO, T. SHONO, T. TAKATSU and H. HOSODA, *Oper. Dent.* **19** (1994) 9.
31. A. I. ABDALLA and C. L. DAVIDSON, *J. Dent.* **24** (1996) 87.
32. H. SANO, M. YOSHIYAMA, S. EBISU, M. F. BURROW, T. TAKATSU, B. CIUCCHI, R. M. CARVALHO and D. H. PASHLEY, *Oper. Dent.* **20** (1995) 160.
33. W. WU, E. COBB and K. DERMANN, *J. Biomed. Mater. Res.* **17** (1983) 37.

34. R. DE SANTIS, P. ANDERSON, K. E. TANNER, L. AMBROSIO, L. NICOLAIS, W. BONFIELD and G. R. DAVIS, *J. Mater. Sci. Mater. Med.* **10** (2000) 629.
35. P. J. DUKE, in ''Synchrotron radiation (Production and Properties)'' (New York, Oxford University Press, 2000).
36. H. J. BESCH, *Nucl. Instr. Meth. Phys. Res.* **A419** (1998) 202.
37. J. L. DRUMMOND, R. L. SAKAGUCHI, D. C. RACEAN, J. WOZNY and A. D. STEINBERG, *J. Biomed. Mater. Res.* **32** (1996) 533.
38. H. SANO, T. SHONO, H. SONODA, T. TAKATSU, B. CIUCCHI, R. M. CARVALHO and D. H. PASHLEY, *Dent. Mater.* **10** (1994) 236.
39. D. H. PASHLEY, H. SANO, B. CIUCCHI, M. YOSHIYAMA and R. M. CARVALHO, *ibid.* **11** (1995) 117.
40. S. PHRUKKANON, M. F. BURROW and M. J. TYAS, *ibid.* **14** (1998) 120.
41. M. F. BURROW, U. NOPNAKEEPONG and S. PHRUKKANON, *ibid.* **18** (2002) 239.
42. A. TAKAHASHI, Y. SATO, S. UNO, P. N. R. PEREIRA and H. SANO, *ibid.* **18** (2002) 263.
43. W. G. MCDONOUGH, J. M. ANTONUCCI, J. HE, Y. SHIMADA, M. Y. M. CHIANG, G. E. SCHUMACHER and C. R. SCHULTHEISZ, *Biomaterials* **23** (2002) 3603.
44. R. B. PRICE, T. DERAND, P. ANDREOU and D. MURPHY, *ibid.* **24** (2003) 1013.
45. H. ENSAFT, D. M. O'DOHERTY and P. H. JACOBSEN, *ibid.* **22** (2001) 97.
46. R. DE SANTIS, D. PRISCO, A. APICELLA, L. AMBROSIO, S. RENGO and L. NICOLAIS, *J. Mater. Sci. Mater. Med.* **4** (2000) 201.
47. S. Y. LEE, H. C. CHIANG, H. M. HUANG, Y. H. SHIH, H. C. CHEN, D. R. DONG and C. T. LIN, *Biomaterials* **22** (2001) 113.
48. P. AUSIELLO, A. APICELLA and C. D. DAVIDSON, *Dent. Mater.* **18** (2002) 295.
49. P. AUSIELLO, A. APICELLA, C. L. DAVIDSON and S. RENGO, *J. Biomech.* **34** (2001) 1269.
50. R. DE SANTIS, D. PRISCO, S. N. NAZHAT, F. RICCITIELLO, L. AMBROSIO, S. RENGO and L. NICOLAIS, *J. Biomed. Mater. Res.* **55** (2001) 629.
51. R. DE SANTIS, F. MOLLICA, L. MANTO, L. AMBROSIO and L. NICOLAIS, in International Conference on Advances of Biomaterials for Reconstructive Medicine, Capri 9–14, June 2002, p. 31.
52. N. P. CHEREMISINOFF, in ''Practical Statistics for Engineers and Scientists'' (Lancaster Technomic Publishing Company Inc. 1987) pp. 71–112.
53. W. WEIBULL, *J. Appl. Mech.* **18** (1951) 293.
54. C. ROBIN, S. S. SCHERRER, H. W. A. WISKOTT, W. G. DE RIJK and U. C. BELSER, *Dent. Mater.* **18** (2002) 189.
55. Y. KUBOKY and G. L. MECHANIC, *Calcif. Tissue Int.* **34** (1982) 306.
56. H. LI, M. F. BURROW and M. J. TYAS, *Dent. Mater.* **16** (2000) 48.
57. J. D. EICK, A. J. GWINNETT, D. H. PASHLEY and S. J. ROBINSON, *Crit. Rev. Oral. Biol. Med.* **8** (1997) 306.
58. K. L. AGEE, E. L. PASHLEY, A. ITTHAGARUN, H. SANO, F. R. TAY and D. H. PASHLEY, *Dent. Mater.* **19** (2003) 60.

Received 4 October
and accepted 10 October 2003